Journal of Materials Chemistry A

Accepted Manuscript

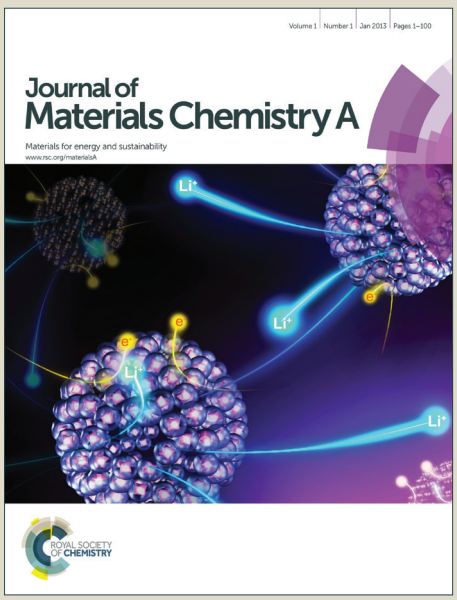

ROYAL SOCIETY OF CHEMISTRY

www.rsc.org/materialsA

Cite this: DOI: 10.1039/c0xx00000x

www.rsc.org/xxxxxx

ARTICLE TYPE

High-performance all solid-state micro-supercapacitor based on patterned photoresist-derived porous carbon electrode and ionogel electrolyte

Shuang Wang,[a,b] Ben Hsia,[a] Carlo Carraro,[a] and Roya Maboudian*[a]

Received (in XXX, XXX) Xth XXXXXXXXX 20XX, Accepted Xth XXXXXXXXX 20XX
DOI: 10.1039/b000000x

We report an all solid-state micro-supercapacitor with patterned photoresist-derived porous carbon electrodes and an ionogel electrolyte. The interdigitated finger electrodes are synthesized via pyrolysis of SPR-220 photoresist, which results in a high surface area porous carbon via a highly scalable technique. The ionogel electrolyte is formed by 1-ethyl-3-methylimidazolium bis(trifluoromethylsulfonyl)imide ionic liquid hybridized with a fumed silica nanopowder. The fabricated device has an excellent long-term cycling stability. The maximum energy density obtained is about 3 mWh cm^{-3}, higher than that of commercial Li-ion thin film batteries, with the maximum achieved power density of 26 Wcm^{-3}. Our results indicate that the novel combination of pyrolyzed photoresist with ionogel electrolyte holds promise for applications in integrated energy storage for all solid-state microsystems or microelectronics technologies.

1. Introduction

Supercapacitors (SCs) have attracted increasing attention because they bridge the energy and power density gap between batteries and capacitors.[1] SCs can be divided into two types based on energy storage mechanism: one is the electrochemical double layer capacitor, which stores energy via ion adsorption at the electrode/electrolyte interface; the other is the pseudocapacitor, which stores energy using surface and near-surface redox reactions.[2]When SCs are miniaturized, they can help to satisfy the increasing energy demand of microdevices, such as autonomous microsensors, micro-robots and implantable medical devices.[3,4,5,6,7] On-chip integration of energy storage devices can achieve high efficiency energy delivery.[8,9]

The electrode materials of SCs must have high specific surface area, which is of utmost importance to achieve high energy densities. Highly porous carbon materials are commonly used as supercapacitor electrodes due to their high specific surface area and good conductivity.[10, 11]Examples of these high surface area materials include onion-like carbon,[5]activated carbons,[12]carbon nanotubes,[13] carbon aerogels,[14] carbide-derived carbon[9, 15] and carbon fibers.[16] In order to realize on-chip integrated micro-supercapacitors, a scalable technique for deposition and patterning of porous carbon material is required. Pyrolyzed photoresist-derived carbon is one attractive electrode material candidate for electrochemical applications owing to its good electrochemical performance and excellent properties including easy fabrication procedure.[17]

The electrolyte, the other core component of SCs, should meet the requirements of high ionic conductivity and wide electrochemical stability window.[18] Conventional SCs typically use a liquid phase electrolyte; however, for micro-supercapacitors, all solid-state devices would significantly simplify the fabrication and packaging processes as well as improve their safety.[19] Ionogels, which maintain the electrochemical properties of ionic liquids and can be easily shaped for the desired applications, have been demonstrated as an effective solid-state electrolyte material with good mechanical compliance and a large electrochemical window.[20, 21, 22]

In this study, an all solid-state micro-supercapacitor based on patterned photoresist-derived porous carbon microelectrodes and ionogel is demonstrated through a combined micro-fabrication and sol-gel approach. The patterned electrode is fabricated through a simple and scalable method that is easily amenable to on-chip integration. The ionogel is obtained by mixing together a fumed silica nanopowder and an ionic liquid.[21] Combining the highly porous patterned electrode and ionogel electrolyte, the all solid-state micro-supercapacitor presented here shows high specific energy and excellent cycling stability.

2. Experimental

2.1 Electrode fabrication

A planar microsupercapacitor configuration is selected in which interdigitated electrodes are fabricated on the same plane and isolated by a physical separation. This configuration has the advantages of easy fabrication and flexibility to the electrolyte choice.[23] Figure 1 (a) shows the device fabrication procedure. The patterned electrodes are fabricated via three primary steps: photoresist deposition, patterning and pyrolysis. A 100-nm thermal oxide is grown on Si (100) wafers to electrically

Cite this: DOI: 10.1039/c0xx00000x

www.rsc.org/xxxxxx

ARTICLE TYPE

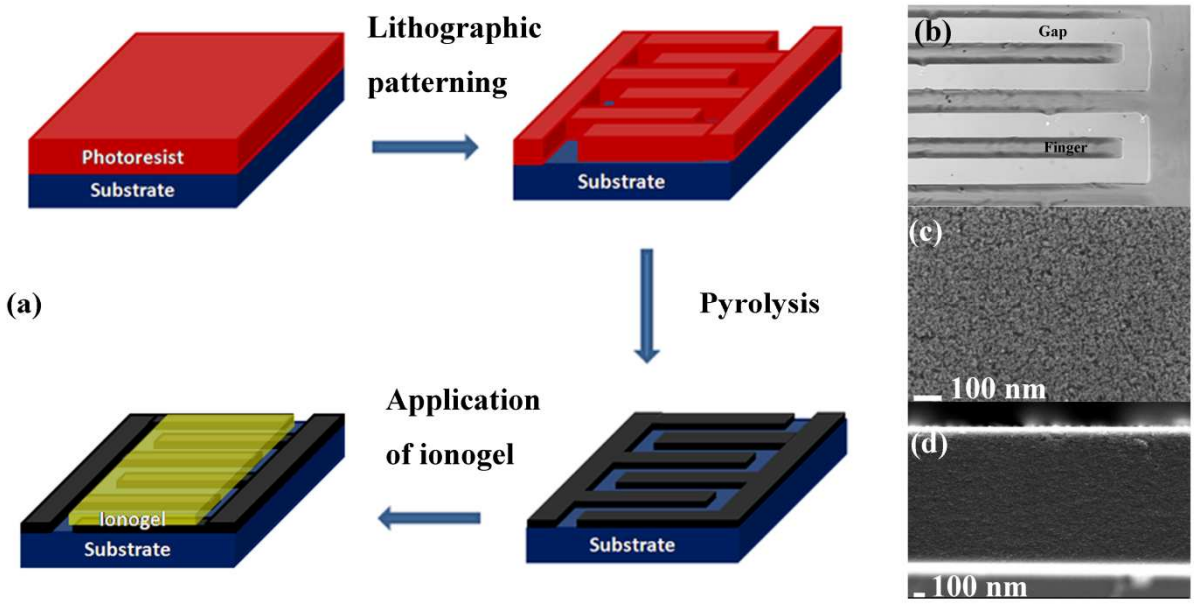

Fig. 1(a) Schematic illustration of micro-supercapacitordevice fabricationprocess; (b) optical image of the patterned photoresist-derived porous carbonlinesafterpyrolysis; (c) SEM top-view and (d) SEM cross-sectional view of a pyrolyzedline.

isolatethe supercapacitor from the substrate. SPR-220-7 photoresist (MicroChem) is spun coat to an approximate thickness of 10 μm on the SiO_2/Si wafer. Following a 5-min soft bake at 115 °C in air, the interdigitated electrodes are patterned via UV lithography. The wafer is diced into individual chips, which are then loaded into a hot-wall chemical vapor deposition furnace (Thermo Scientific Lindberg Blue M). After purging for several minutes in Ar, the furnace is heated to 300 °C and held at this temperature for 30 min under ~1 Torr Ar. The temperature is then increased at a rate of ~30 °C min^{-1} to 900 °C; at this temperature, the ambient gas is switched to a H_2/Ar mixture (10%/90%, Praxair) and the temperature is held for 1 h. Finally, the sample is cooled at a rate of about 25 °C min^{-1} to room temperature in the same H_2/Ar gas environment. For electrochemical testing, silver epoxy is used to electrically contact the patterned electrodes to Cu wires.

2.2 Ionogel preparation

The ionogel electrolyte used in this study is prepared following closely the procedure in Ref. 21, with the gelation mechanism described in Ref. 24. A fumed silica nanopowder (FS, Sigma-Aldrich, 7 nm) and 1-ethyl-3-methylimidazolium bis(trifluoromethylsulfonyl)imide (EMI TFSI, Iolitec, 99% purity) are used without further purification. The FS and EMI TFSI are mixed in a 0.03:1 mass ratio in a glass vial. The mixture is stirred for 5 min to ensure the solution is uniformly mixed. The solution is then transferred via a micropipette onto the patterned electrode and allowed to gel in a nitrogen rich, low-humidity (<1% relative humidity) environmental chamber. The gelation process takes about 12 h to complete.

2.3 Characterization methods

Porous carbon morphology is characterized by scanning electron microscopy using a Zeiss Gemini Ultra-55 analytical SEM. Electrochemical testing is performed using a potentiostat (CH Instruments, 660D Model). The samples are kept in a low-humidity environmental chamber during testing. Cyclic voltammetry (CV) is used to determine specific capacitance. A potential window of 2V is used and various scan rates (ranging from 0.01 to 20V s^{-1}) are applied. Constant-current charge and discharge cycles are performed to quantify the equivalent series resistance (ESR) of the device.[25] In order to probe the frequency response of the device, AC impedance spectroscopy (potential amplitude of 5 mV) is performed. Long-term cycling stability is investigated via repetitive CV scans at the full potential window of 2 V at a scan rate of 0.5 V s^{-1}.

3. Results and discussion

3.1 Structural characterization

The microsupercapacitor reported here consists of two interdigitated electrodes, each having 9 fingers with size 0.250 ×

Cite this: DOI: 10.1039/c0xx00000x

www.rsc.org/xxxxxx

ARTICLE TYPE

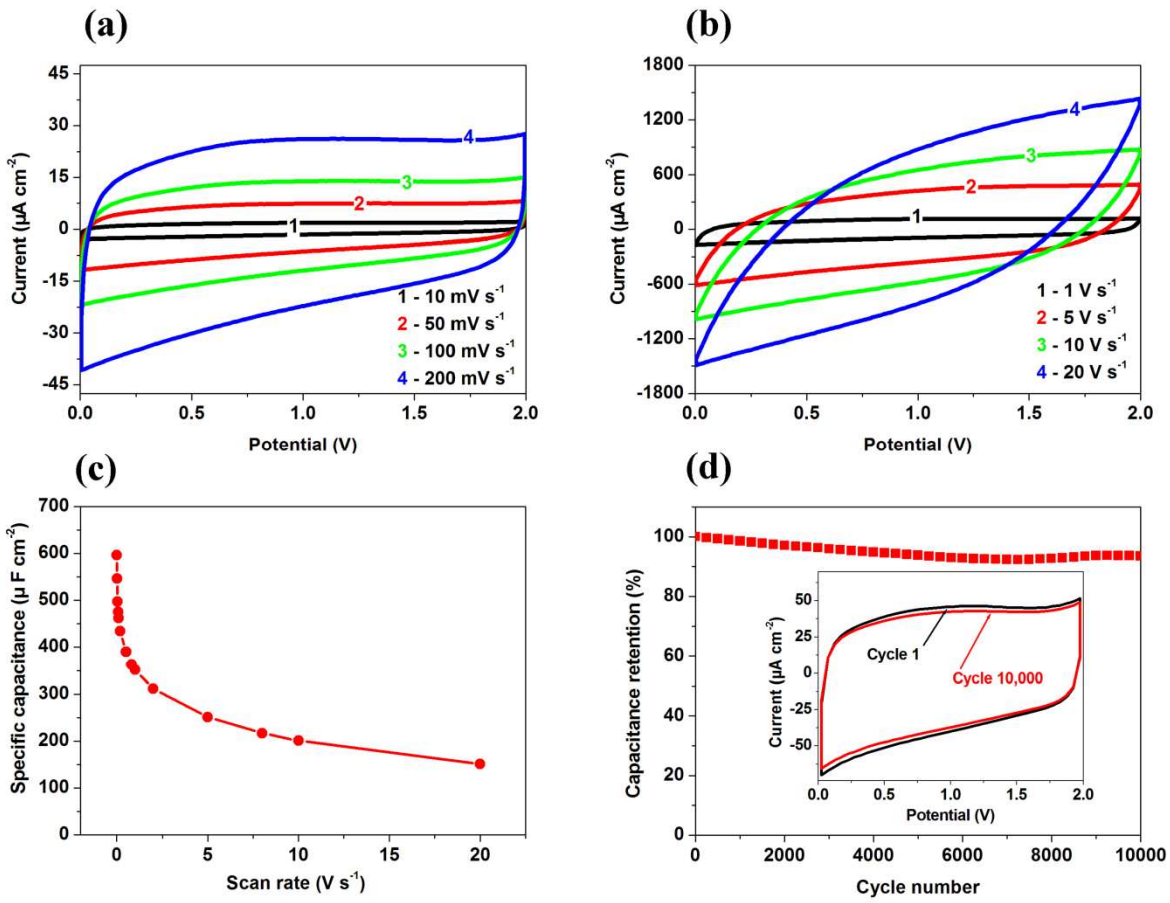

Fig. 2(a-b) Cyclic voltammograms of the fabricated micro-supercapacitor at various voltage scan rates; (c) Specific capacitance dependence on scan rates; and (d) Lifetime testing of the fabricated device. Capacitance is plotted over 10,000 cyclic voltammograms cycles, normalized by original capacitance value. Scan rate is 0.5 V s^{-1} and voltage window is 2 V. The CV plots of the first cycle and the 10,000th cycle are provided in the inset.

6 mm^2, and a gap between fingers of 300μm. An optical image of the microfabricated porous carbon electrode, showing three full fingers, is provided in Fig.1 (b). Figures 1 (c) and (d) show representative top- and cross-sectional view SEM images of the pyrolyzed finger, respectively. As reported previously via high-resolution imaging and Raman spectroscopy,[17] the pyrolysis process yields high surface area graphitic carbon. The thickness of the pyrolyzed fingers decreases from ~10 μm during the pyrolysis to 1.2 μm; however, the footprint of the electrode remains approximately the same due to good adhesion with the underlying substrate.

3.2 Cyclic voltammetry and long-term cycling stability

Figures 2 (a) and (b) show the current vs. voltage applied between the two electrodes over a 2V potential window at scan rates ranging from 10 mV s^{-1} to 20 V s^{-1}.The specific capacitance (C) can be calculated via the equation,

$$C = \frac{I_{avg}}{sA} \quad (1)$$

where I_{avg} is the average current magnitude of the cathodic and anodic sweeps, s is the voltage scan rate and A is the total electrode area covered by the ionogel, measured to be about 0.225 cm^2. At low scan rates, the CV curves show a quasi-rectangular shape, with an increasing cathodic current at low potentials. A rectangular CV curve would indicate pure double layer capacitance. The observed deviation from a rectangular shape indicates the occurrence of electrode/electrolyte charge transfer which could arise from reactions occurring at the electrodes, in the electrolyte, or both. These reactions can be considered pseudocapacitive if the charge transfer is reversible, as reversible surface reactions can contribute to additional charge storage. [26] Previous investigations on pyrolyzed photoresist

Cite this: DOI: 10.1039/c0xx00000x

www.rsc.org/xxxxxx

ARTICLE TYPE

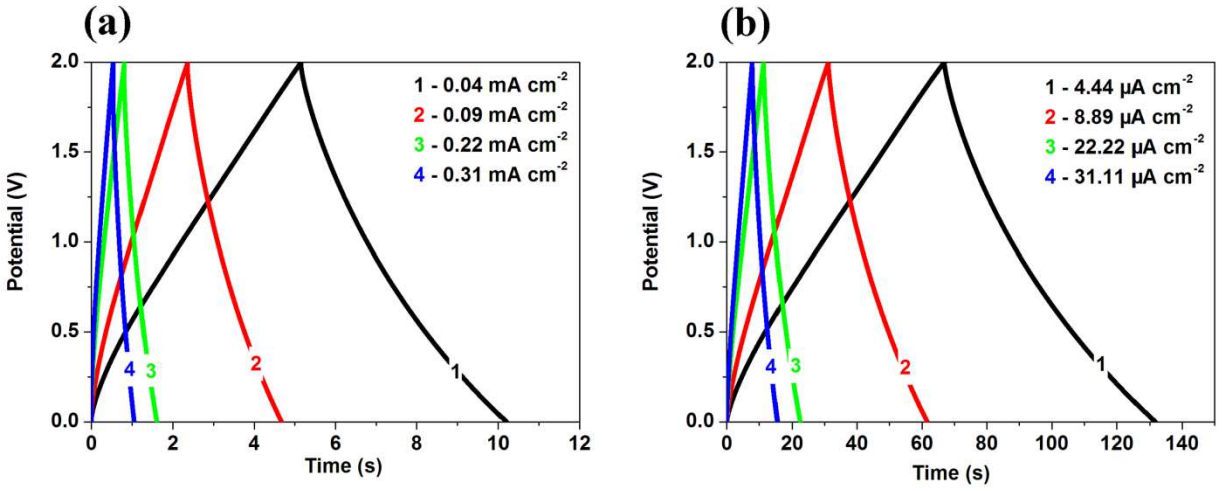

Fig. 3(a, b) Galvanostatic charge/discharge curves for the fabricated micro-supercapacitor for a variety of specific currents.

electrodes in a three-electrode setup in aqueous electrolyte also showed evidence of pseudocapacitive reactions in aqueous electrolytes, which were attributed to the reversible reaction of surface oxygen-containing functional groups on the electrode.[27] Of course, pseudocapacitive contributions are useful only if the reactions do not adversely affect the long-term performance of the device. At higher scan rates, the CV curves become skewed and the voltammogram edges round off, resulting in a decrease in capacitance. These characteristics arise from internal resistances including the electrical resistivity (120 Ω cm) of the pyrolyzed photoresist film and the resistance to ionic transport in the electrolyte and in the porouselectrode.[16, 28] This effect of scan rate on capacitance is clearly illustrated in Fig. 2 (c), which plots the specific capacitance as a function of scan rate. The specific capacitance drops rapidly (from 600 to 150 μFcm^{-2}) with scan rate increasing from 0.01 to 2 V s^{-1}, but then drops more slowly with the scan rate further increasing from 2 to 20 V s^{-1}.

A long-term cycling stability test is performed via repetitive CV scans over the full 2V voltage window at a scan rate of 0.5 V s^{-1}. Figure 2 (d) shows the percent retained capacitance as a function of the cycle number. The micro-supercapacitor retains 94% of its initial capacitance after 10,000 cycles, which reveals a stable behavior for the electrode material and ionogel electrolyte. The inset shows the first cycle and the 10,000th cycle CV scans, and clearly demonstrates that the CV shape is unchanged after long-term cycling. Moreover, the cathodic current at low potentials also remains the same; thus, the charge transfer reactions do not have a negative effect on the stability of the fabricated device and can be considered to contribute to pseudocapacitive charge storage. The charge stored during charging and delivered during discharging are measured to show a deviation of only about 0.5%, confirming the reversibility of the charge transfer reactions. The small drop (6%) in capacitance seen upon cycling is typical of many supercapacitor devices reported in literature. [29, 30]

3.3 Galvanostatic charge/discharge

Galvanostatic charge/discharge of the fabricated device are performed at a variety of specific currents and the curves are presented in Fig.3. Pseudolinear discharge curves are observed for all tested currents. The device equivalent series resistance can be estimated using the magnitude of the IR drop, [21] and is calculated to be ~ 650 Ωcm^{-2} electrode area at various current densities ranging from about 4 to 310 μA cm^{-2}. Such large values of ESR likely contribute to the sharp decrease in capacitance with increasing scan rate seen in the CV results. The nonlinearity of the discharge curve results from the charge transfer reactions discussed in the previous section. Given the excellent CV cycling stability of the device, this nonlinearity is not expected to have an adverse effect on the device performance.

3.4 AC impedance spectroscopy

Figure 4 shows the AC impedance spectroscopy results for the fabricated device. From the *x*-intercept of the Nyquist plot shown in Fig. 4 (a), the equivalent series resistance can be obtained, [31,32] The ESR is found to be 740 Ωcm^{-2} electrode area from this analysis, in reasonable agreement with the galvanostatic charge/discharge results. Regarding the shape of the Nyquist curve, an ideal RC circuityields a vertical line, with the *x*-intercept representing the ESR. It is known that porous geometries typically lead to a high-frequency semicircle, due to the high resistance to ionic transport in small pores. [33] Studies on pyrolyzed photoresist under these conditions show a high for frequency semicircle in three-electrode AC impedance tests.[16] High-frequency semicircles have also been frequently reported on

Cite this: DOI: 10.1039/c0xx00000x

www.rsc.org/xxxxxx

ARTICLE TYPE

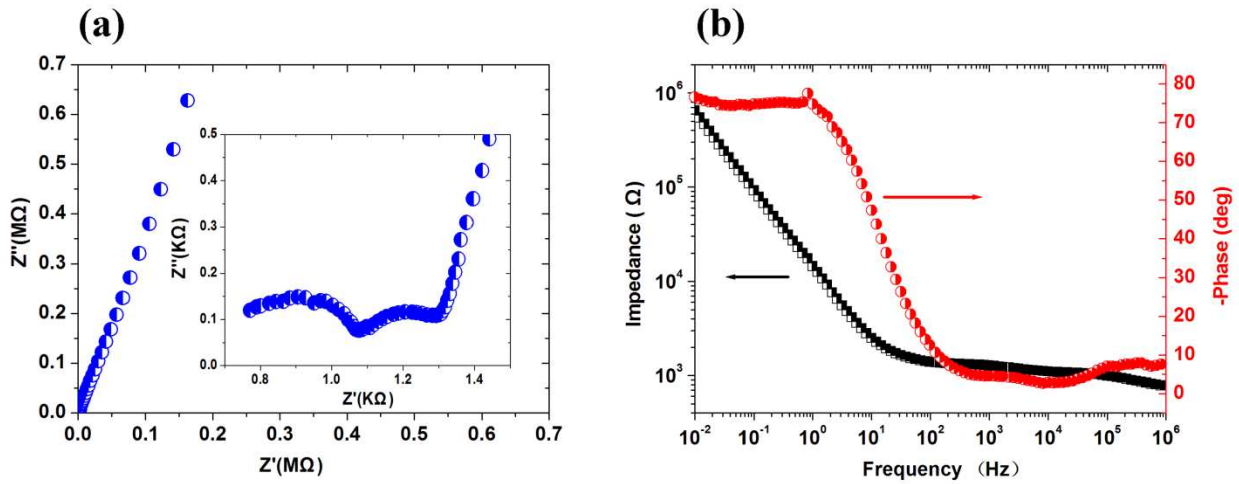

Fig. 4AC impedance data showing the (a) Nyquist plot with an enlarged view of the high-frequency region provided in the inset and (b) Bode plots

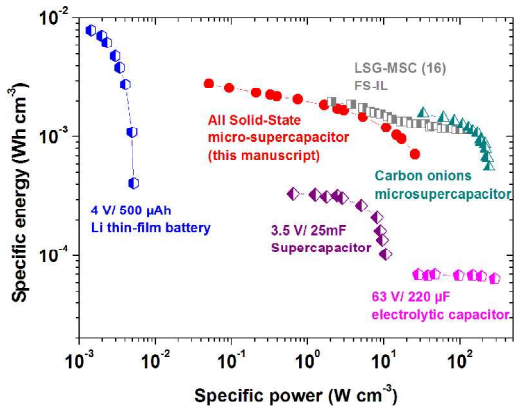

Fig. 5 Ragone plot of the specific energy and power density (per cm^3 of electrode volume) of the all solid-state micro-supercapacitorand other microdevices. Data forlaser-scribed graphene (LSG-MSC16), carbon onions micro-supercapacitorand other commercial devices (Li thin-film battery, 3.5V/25mF supercapacitor and 63V/220 µF electrolytic capacitor) obtained from Ref. 9 and 21, respectively.

pseudocapacitive reactions that are limited by charge transfer and kinetics. [34, 35] The CV and galvanostatic charge/discharge results clearly show the presence of charge transfer reactions at the electrodes, and hence the presence of a second high frequency semicircle is expected. While definitive assignment of each arc to a particular phenomenon is not possible given the probed data, the AC impedance behavior nonetheless confirms the interpretation of the CV and galvanostatic charge/discharge results. Figure 4 (b) displays the Bode plots of the fabricated supercapacitor. The frequency at the phase angle of -45° (f_0), defined as the onset of capacitive behavior, is about 11 Hz, to be compared to that of onion-like carbon (38 Hz), [5]activated carbon (1 Hz). [5] Pure capacitive behavior can be obtained and most of the stored energy is accessible at frequencies below this frequency. [5,36, 37]

3.5 Energy and power density

For practical energy storage devices, high energy and power density are necessary. Generally, there is a trade-off between energy density and power density in electrochemical energy storage devices. The theoretical energy, E, and power density, P, in supercapacitors can be calculated via Eqs.2 and 3.

$$E = \frac{1}{2}CV^2 \quad (2)$$

$$P = \frac{E}{\Delta t} \quad (3)$$

where C is the specific capacitance, V is the maximum voltage window and Δt is the discharge time. Using the electrode volume to calculate the specific capacitance yields a volumetric energy density value ranging from 0.7 to 3 mWh cm^{-3} with a maximum power density of about 26 W cm^{-3}. Figure 5 shows a Ragone plot of the specific energy vs. power density for the fabricated device. Neither thin film lithium-ion batteries nor conventional supercapacitors can provide the high energy and power density of the device presented here.[9] The specific energy density of the fabricated device in this work is comparable with that of onion-like carbon micro-supercapacitors and laser scribed graphene (LSG) micro-supercapacitors. [9, 22]

4. Conclusion

In conclusion, an all solid-state micro-supercapacitor is successfully fabricated using microfabricated photoresist-derived porous carbon electrodes with an ionogel electrolyte. The

electrode synthesis method is simple and scalable and the electrode can be readily patterned, leading to easy integration in an on-chip micropowerdevice. The fabricated device has excellent long-term stability and yields high energy and power performance. This novel combination of electrode materials and solid-state ionogel electrolyte shows significant promise for microdevice energy storage applications.

Acknowledgments

We gratefully acknowledge the China Scholarship Council Fellowship #201206170078 (SW), National Science Foundation through a Graduate Research Fellowship (BH) and through Center of Integrated Nanomechanical Systems and the Siemens CKI program for supporting this work.

Notes and references

[a]*Department of Chemical and Biomolecular Engineering, University of California, Berkeley, California, 94720-1462, USA Fax: +1 510 642 4778; Tel: +1 510 643 7957; E-mail: maboudia@berkeley.edu*
[b]*Alan G. MacDiarmid Institute, College of Chemistry, Jilin University, Changchun, 130012, CHINA. E-mail: w.shuang25@gmail.com*

1 P. Simon and Y. Gogotsi, *Nat. Mater.*, 2008, 7, 845-854.
2 M. Beidaghi and C. Wang, *Electrochim. Acta*, 2011, 56, 9508-9514.
3 J-H. Sung, S-J. Kim, S-H. Jeong, E. H. Kim and K-H. Lee, *J. Power Sources*, 2006, 162, 1467-1470.
4 M. Kaempgen, C. K. Chan, J. Ma, Y. Cui and G. Gruner, *Nano Lett.*, 2009, 9, 1872-1876.
5 D. Pech, M. Brunet, H. Durou, P. Huang, V. Mochalin, Y. Gogotsi, P-L. Taberna and P. Simon, *Nat. Nanotechnol.*, 2010, 5, 651-654.
6 M. Armand and J. M. Tarascon, *Nature*, 2008, 451, 652-657.
7 S. D. Jones and J. R. Akridge, *Solid State Ionics*, 1996, 86-88, 1291-1294.
8 K. Wang, W. Zo, B. Quan, A. Yu, H. Wu, P. Jian and Z. Wei, *Adv. Energy Mater.*, 2011, 1, 1068-1072.
9 J. Chmiola, C. Largeot, P. L. Taberna, P. Simon and Y. Gogotsi, *Science*, 2010, 328, 480-483.
10 A. G. Pandolfo and A. F. Hollenkamp. *J. Power Sources*, 2006, 157, 11-27.
11 E. Frackowiak, *Phys. Chem. Chem. Phys.*, 2007, 9, 1774-1785.
12 Y. Kibi,T. Saito, M. Kurata, J. Tabuchi and A. Ochi, *J. Power Sources*, 1996, 60, 219-224.
13 E. Frackowiak, K. Metenier, V. Bertagna and F. Beguish, *Appl. Phys. Lett.*, 2000, 77, 2421-2423.
14 S. T. Mayer, R. W. Pekala and J. L. Kaschmitter, *J. Electrochem. Soc.*, 1993, 140, 446-451.
15 F. Liu, A. Gutes, I. Laboriante, C. Carraro and R. Maboudian, *Appl. Phys. Lett.*, 2011, 99, 112104-112104-3.
16 H. Nagawa, A. Shudo and K. Miura, *J. Electrochem. Soc.*, 2000, 147, 38-42.
17 B. Hsia, M-S. Kim, M. Vincent, C. Carraro and R. Maboudian, *Carbon*, 2013, 57, 395-400.
18 Y-S. Ye, J. Rick and B-J. Hwang, *J. Mater. Chem. A*, 2013, 1, 2719-2743.
19 D. Wei, S. J. Wakeham, T. W. Ng, M. J. Thwaites, H. Brown and P. Beecher, *Electrochem. Commun.*, 2009, 11, 2285-2287.
20 J. L. Bideau, L. Viaub and A. Vioux. *Chem. Soc. Rev.*, 2011, 40, 907-925.
21 M. F. El-Kady and R. B. Kaner, *Nat. Commun*, 2013, 4, 1475-1483.
22 B. Hsia, S. Wang, M-S. Kim, C. Carraro and R. Maboudian, Proceedings of the 16th International Conference on Solid-State Sensors and Actuators, Transducers '13, 2013, pp. 1328-1331.
23 D. Pech, M. Brunet, T-M. Dinh, K. Armstrong, J. Gaudet and D. Guay, *J. Power Sources*, 2013, 230, 230-235.
24 X.-J. Wu, Y. Wang, W. Yang, B.-H. Xie, M.-B. Yang and W. Dan, Soft Mater., 2012, 8, 10457-10463.
25 M. D. Stoller and R. S. Ruoff, *Energ. Environ. Sci.*, 3 (2010) 1294-1301.
26 B. E. Conway, V. Birss and J. Wojtowicz, *J. Power Sources*, 1997, 66, 1-14.
27 B. Hsia, M-S. Kim, C. Carraro and R. Maboudian, *J. Mater. Chem A*, 2013, 1, 10518-10523.
28 J. Lin, C. Zhang, Z. Yan, Y. Zhu, Z. Peng, R. H. Hauge, D. Natelson and J. M. Tour, *Nano Lett.*, 2013, 13, 72-78.
29 A. Balducci, W. A. Hendersonc, M. Mastragostinoa, S. Passerinic, P. Simonb and F. Soavi, *Electrochim.Acta*, 2005, 50, 2233-2237.
30 Y. Chen, X. Zhang, D. Zhang, P. Yu and Y. Ma, *Carbon*, 2011, 49, 573-580.
31 E. Barsoukov and J. R. Macdonald, Impedance Spectroscopy: Theory, Experiment, and Applications, John Wiley, New Jersey 2005.
32 M. D. Stoller, S. J. Park, Y. W. Zhu, J. H. An and R. S. Ruoff, *Nano Lett.*, 2008, 8, 3498-3502.
33 C. Hitz and A. Lasia, *J. Electroanal. Chem.*, 2001, 500, 213-222.
34 M-K. Song, S. Cheng, H. Chen and M. Liu, *Nano Lett.*, 2012, 12, 3483-3490.
35 Y. Yun, M. Lee, M. Joo and H-J. Jin, *J. Power Sources*, 2014, 246, 540-547.
36 M. Toupin, T. Brousse and D. Bélanger, *Chem. Mater.*, 2004, 16, 3184-3190.
37 L. Yuan, X. Lu, X. Xiao, T. Zhai, J. Dai, F. Zhang, B. Hu, X. Wang, L. Gong, J. Chen, C. Hu, Y. Tong, J. Zhou and Z. Wang, *ACS Nano*, 2012, 6 (1), 656-661.

High-performance all solid-state micro-supercapacitor based on patterned photoresist-derived porous carbon electrode and ionogel electrolyte

Shuang Wang,[a,b] Ben Hsia,[a] Carlo Carraro,[a] and Roya Maboudian*[a]

An all solid-state micro-supercapacitor is fabricated using patterned photoresist-derived porous carbon electrodes and an ionogel electrolyte. The fabricated device has excellent long-term stability and yields high energy and power performance.

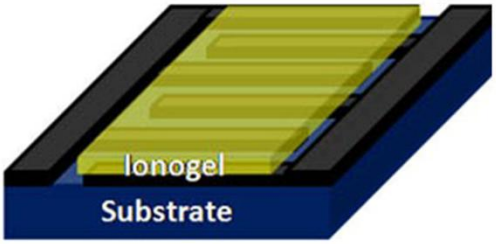

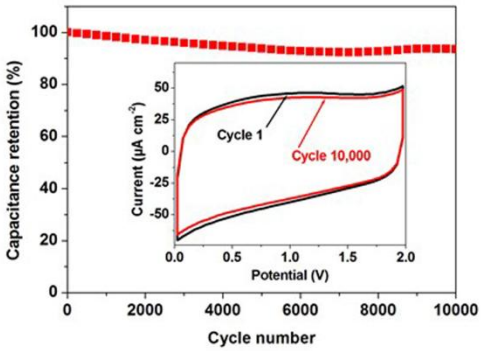

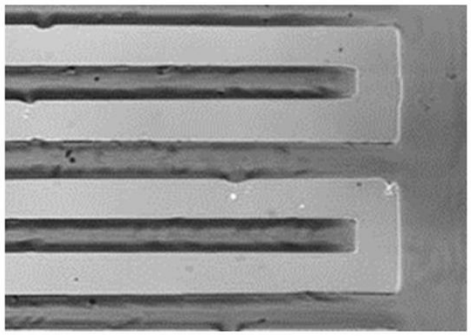

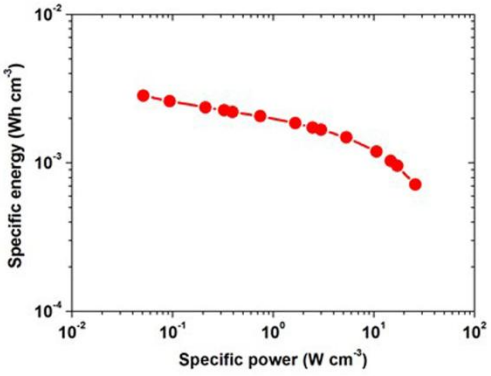

An all solid-state micro-supercapacitor is fabricated using patterned photoresist-derived porous carbon electrodes and an ionogel electrolyte. The fabricated device has excellent long-term stability and yields high energy and power performance.